Published in final edited form as:
Mol Cancer Ther. 2013 July ; 12(7): 1245–1254. doi:10.1158/1535-7163.MCT-12-1150.

Fibroblast Growth Factor Receptor 3 is a Rational Therapeutic Target in Bladder Cancer

Kilian M. Gust[1], **David J. McConkey**[2], **Shannon Awrey**[1], **Paul K. Hegarty**[2], **Jing Qing**[3], **Jolanta Bondaruk**[2], **Avi Ashkenazi**[3], **Bogdan Czerniak**[2], **Colin P. Dinney**[2], and **Peter C. Black**[1]

[1]Vancouver Prostate Centre, Department of Urologic Sciences, University of British Columbia, Vancouver, BC, Canada

[2]The University of Texas, MD Anderson Cancer Center, Houston, TX, USA

[3]Department of Molecular Oncology, Genentech Inc., South San Francisco, CA, USA

Abstract

Activating mutations of Fibroblast growth factor receptor-3 (FGFR3) have been described in approximately 75% of low-grade papillary bladder tumors. In muscle invasive disease, FGFR3 mutations are found in 20% of tumors, but overexpression of FGFR3 is observed in about half of cases. Therefore, FGFR3 is a particularly promising target for therapy in bladder cancer. Up to now most drugs tested for inhibition of FGFR3 have been small molecule, multi-tyrosine kinase inhibitors. More recently, a specific inhibitory monoclonal antibody targeting FGFR3 (R3Mab) has been described and tested pre-clinically. In this study, we have evaluated mutation and expression status of FGFR3 in 19 urothelial cancer cell lines and a cohort of 170 American bladder cancer patients. We demonstrated inhibitory activity of R3Mab on tumor growth and corresponding cell signaling in three different orthotopic xenografts of bladder cancer. Our results provide the pre-clinical proof of principle necessary to translate FGFR3 inhibition with R3Mab into clinical trials in patients with bladder cancer.

Keywords

bladder cancer; FGFR3; targeted therapy; orthotopic xenograft model; monoclonal antibody

Introduction

Cancer of the bladder will be newly diagnosed in an estimated 73,510 individuals and will cause 14,880 cancer related deaths in 2012 in the United States (1). This makes it the fourth most common cancer in men and the ninth most common in women. About 70% of cases are non-muscle invasive and have a high propensity to recur, giving bladder cancer the highest recurrence rate of any cancer (2). This translates clinically into intensive surveillance and multiple interventions over many years, explaining the high cost of managing bladder cancer (3). The other 30% of cases are muscle invasive tumors, for which the five-year survival is

Corresponding author: Peter C. Black Vancouver Prostate Centre Department of Urologic Sciences University of British Columbia 2660 Oak Street Vancouver, BC V6H 3Z6 Canada Fax +1 (604) 875-5654 Phone +1 (604) 875-4818 pblack@mail.ubc.ca.

Potential conflict of interest: Jing Qing has ownership interest in Genentech Inc.
Avi Ashkenazi is employee of Genentech Inc.
David J. McConkey has a commercial research grant (Astra-Zeneca; ownership interest for patent from Apocell, Inc. and is consultant an on advisory board of Apocall, Inc.
None of the other authors declare any potential conflict of interest.

approximately 50%. Both disease entities are marked by a paucity of new discoveries leading to novel therapies with clinical utility.

Fibroblast growth factor receptor-3 (FGFR3) is a particularly promising target for therapy in bladder cancer. Activating FGFR3 mutations have been described in approximately 75% of low-grade papillary bladder tumors (4). Mutations are found in only 20% of muscle invasive tumors, but FGFR3 over-expression is observed in 50% of these tumors (5, 6). The most common mutation (S249C), located on exon 7, results in the substitution of serine at codon 249 with a cysteine residue (7, 8). This leads to constitutive ligand-independent dimerization of the receptor and activation of downstream proliferative pathways (9, 10).

Recently a number of small molecule receptor tyrosine kinase inhibitors have been developed to target FGFR3 (11). These small molecule inhibitors, including BGJ398 (Novartis), TKI258/CHIR258 (Dovitinib, Novartis) (12-14), AZD4547 (Astra Zeneca) PD173074 (Pfizer, Groton, CT), and BMS-582664 (Brivanib, Bristol Myers Squibb) (15), generally target all members of the FGFR family, VEGFR2 and other tyrosine kinases (11, 12). This general FGF and VEGF pathway inhibition is associated with significant diarrhea, nausea, fatigue (16, 17), dyspnea (18), and abdominal pain (16-18), as well as thrombocytopenia and thromboembolic events (16). Hyperphosphatemia-mediated soft tissue calcification has been a further hurdle impeding preclinical development of pan-FGFR inhibitors (11). The FGFR pathway is involved in normal phosphate and vitamin D homeostasis, particularly through FGF23 signaling in the bone and kidney (19). Disruption of this pathway with pan-FGFR inhibitors leads to hyperphosphatemia and deposit of calcium phosphorous in the soft tissues, including the vasculature, smooth muscle, and renal tubules. These adverse effects may be avoided with specific FGFR3 inhibition.

The clinical development of these inhibitors has focused on multiple myeloma, which harbors specific translocations (t(4;14)(p16;q32)) that activate FGFR3 (20), and on hepatocellular carcinoma (12), but little work has been done in bladder cancer. Most recently, an inhibitory monoclonal antibody targeting FGFR3 specifically (R3Mab) has been developed and undergone preliminary testing in pre-clinical subcutaneous models of bladder cancer, where it has demonstrated activity on both wild type and mutated FGFR3 (21). In this study, we have focused on specific FGFR3 inhibition with R3Mab in an orthotopic bladder cancer model. The orthotopic model provides an appropriate organ-specific microenvironment that should allow better translation into clinical trials.

Therefore, we aimed to demonstrate the pre-clinical proof of principle that targeting FGFR3 with R3Mab is rational in bladder cancer. We have measured FGFR3 mutation and expression in an American cohort of patients with bladder cancer and have demonstrated R3Mab activity in an orthotopic xenograft model of bladder cancer. We believe that this justifies the translation of FGFR3 inhibition with R3Mab into clinical trials in patients with bladder cancer.

Materials and Methods

Cell lines

A panel of 19 human bladder cancer cell lines was kindly provided by the Pathology Core of the Bladder Cancer SPORE at MD Anderson Cancer Center, including UM-UC1, UM-UC3, UM-UC4, UM-UC5, UM-UC6, UM-UC7, UM-UC10, UM-UC11, UM-UC12, UM-UC13, UM-UC14, UM-UC15, UM-UC16, UM-UC17, 253J-P, 253J-BV, RT4v6 and RT112. T24 was purchased from the American Type Tissue Collection (ATTC, Rockville, MD, USA). All cell lines were cultured in MEM medium, supplemented with 10% FBS, 1% non-essential amino acids, 1% L-glutamine and 1% sodium pyruvate (all purchased from

Invitrogen, Grand Island, NY). Cell lines were routinely grown and passaged at 37°C in a humidified atmosphere of 5% CO_2. Cell line identities were confirmed by DNA fingerprinting using the AmpFlSTR Identifiler Amplification (Applied Biosystems, Carlsbad, CA) or AmpFlSTR Profiler PCR Amplification (Applied Biosystems) protocols. Cell lines were monitored regularly for mycoplasma infection.

For *in vivo* studies, UM-UC1, UM-UC14 and RT112 cell lines underwent transduction with a lentiviral construct carrying the luciferase firefly gene for *in vivo* imaging. The luciferase plasmid contained a blasticidin resistance gene enabling positive selection with 10ug/ml blasticidin (Invitrogen). Cell lines were controlled for *in vitro* luciferase activity and cell number was correlated with bioluminescence (R>0.99; data not shown), using the Xenogen IVIS Spectrum (Caliper Lifesciences, Hopkinton, MA, USA). These three cell lines were chosen due to their high levels of FGFR3 expression and their growth characteristics in the orthotopic xenograft model.

Antibodies

FGFR3 polyclonal (sc-123), FRS2a (sc-8318), Cyclin D1 (sc-718), Cyclin E (sc-481) and Vimentin (sc-5565) antibodies were purchased from Santa Cruz Biotechnologies (Santa Cruz, CA). Antibodies detecting p-FGFR (#3471), p-FRS2 (#3864), p42/44MAPK (#4965), phospho-p42/44-MAPK (#4370), AKT (#9272), phosphor-AKT (ser 473; # 9271S), ZEB-1 (#3396), and cleaved caspase-3 (#9661) were purchased from Cell Signaling (Danvers, MA). Anti-phospho-tyrosine 4G10 was obtained from EMD Millipore (Bedford, MA) and E-cadherin antibody (#610181) from BD Biosciences (Mississauga, ON). A monoclonal Ki-67 antibody for evaluation of proliferation of xenograft tumors was purchased from Thermo Scientific (Waltham, MA). For expression analysis of FGFR3 on the human tissue microarray, a polyclonal FGFR3 antibody (F0425) was obtained from Sigma-Aldrich (St. Louis, MO).

Immunohistochemistry

Use of all human tissue was approved by the Institutional Review Board at MD Anderson Cancer Center and written consent was obtained from all patients. Paraffin–embedded sections of bladder were cut to 4mm and placed on polysine coated microscope slides and baked overnight at 50°C in a dry oven. Sections were then deparaffinized in xylene for 2 × 5minutes and rehydrated in alcohol for 2 × 5 minutes. Endogenous peroxidase activity was quenched by applying 2% hydrogen peroxide in 30% methanol for 10 minutes. Antigen retrieval was performed by incubation in proteinase K (40ug/ml PBS) for 15 minutes at 37°C in a humidified chamber. Sections were stained with primary antibody (Sigma Aldrich) overnight at 4°C. The bound primary antibodies were visualized by avidin-biotin complex assay (DAKO Corp., Carpenteria, CA) with 3,3′-diaminobenzidine as a chromagen (DAKO) and hematoxylin as a counterstain. FGFR3 staining was indicated by characteristic brown staining. Sections from 4 normal human ureters were used as negative control. Staining intensity was assessed on a scale from 0 (no staining) to 3 (strong staining) by a pathologist (B.C.).

FGFR3 mutation analysis

DNA was isolated from the urothelial carcinoma cells and tumor samples using a genomic DNA extraction kit (Qiagen, Bothell, WA) according to the manufacturers' instructions. Exons 7 and 10 were amplified by PCR using AmpliTaq Gold DNA polymerase (Applied Biosystems). The following primers were used: 5′-CGGCAGTGGCGGTGGTGGTG-3′ (sense) and 5′-AGCACCGCCGTCTGGTTGGC-3′ (antisense) for exon 7 (22), and 5′-CCTCAACGCCCATGTCTTT-3′ (sense) and 5′-AGGCAGCTCAGAACCTGGTA-3′ (antisense) for exon 10 (Sigma-Aldrich, St. Louis, MO). Five picomoles of each primer were

added to the 20-μL reaction volume, and 1 μL DMSO was added for exon 7. The following cycling variables were used: 95°C for 10 minutes, then 35 cycles of 95°C for 30 seconds, 65°C (exon 7) or 58°C (exon 10) for 30 seconds, and 72°C for 30 seconds, followed by a final incubation at 72°C for 10 minutes (22). Unincorporated primers and deoxynucleotides were removed using shrimp alkaline phosphatase and exonuclease I (U.S. Biochemical, Cleveland, OH). Direct sequencing was carried out with Big Dye Terminator Cycle Sequencing and the data were analyzed with Sequencing Analysis 3.0 software (Applied Biosystems). Visual inspection of the electropherograms was conducted using Sequence Scanner Software v1.0 (Applied Biosystems). Mutation analysis was verified independently by Dr. François Radvanyi, Ph.D. (Institut Curie, Paris).

Proliferation assay

Proliferation was assessed using the crystal violet assay, as described previously (23). Cells were treated with varying concentrations of R3Mab for 48 to 72 hours. The absorbance was determined with a microculture plate reader (Epoch, BioTek, Winooski, VT) at 562 nm. Cell survival after treatment was calculated as the percentage of absorbance relative to controls.

Western blot analysis

Total protein was isolated with radio-immuno-precipitation buffer (RIPA) supplemented with proteinase- and phosphatase inhibitor for 2 hours on ice. Samples were spun at 13.000 rpm for 20 min, supernatants transferred into empty Eppendorf tubes and protein concentrations measured using the BCA protein assay (Thermo Scientific). 30μg of protein was then run on 8-12% SDS polyacrylamide gels and electrophoretically transferred to Immobilon-P membranes (Millipore). Blots were blocked with Odyssey blocking buffer for 1 hour at room temperature and incubated in primary antibody at 4°C overnight. After washing in TBS-T (TBS with 0.1% Tween 20), membranes were incubated with horseradish peroxidase-conjugated secondary antibody IgG (Santa Cruz Biotechnologies) at 1:5000 dilution for 1 hour. Blots were developed using an enhanced chemiluminescence (ECL) substrate system for detection of horseradish peroxidase, SuperSignal West Femto Maximum Sensitivity Substrate (Thermo Scientific). Immunoprecipitation was performed using a 2 ug FGFR3 polyclonal antibody on 500ug of lysate using the ExactaCruz B system (Santa Cruz).

Real-time PCR analysis

RNA was extracted from cell lines using TRIZOL (Invitrogen, Life Technologies) followed by reverse transcription cDNA generation using the Transcriptor First Strand cDNA Synthesis Kit (Roche, Mississauga, Ont). Quantitative real time monitoring of FGFR3 receptor and EMT markers expression was performed in triplicates on the ABI PRISM 7900 Sequence Detection System (Applied Biosystems) using FastStart Universal SYBR Green Master Mix with Rox (Roche) under universal cycling conditions. Relative target gene expression was normalized to glyceraldehyde-3-phosphate dehydrogenase (GAPDH) levels as an internal control by the comparative cycle threshold (ΔCt) method. Relative expression amongst the panel of cell lines was expressed compared to epithelial cancer cell line RT4v6 for FGFR3 and to mesenchymal cell line 253J-BV for EMT markers. Following 5′ to 3′ primer pairs were used: ZEB-1 Fwd GCA CCT GAA GAG GAC CAG AG, Rev TGC ATC TGG TGT TCC ATT TT, E-Cadherin Fwd AGA ACG CAT TGC CAC ATA CAC TC, Rev CAT TCT GAT CGG TTA CCG TGA TC, Vimentin Fwd ACA CCC TGC AAT CTT TCA GAC A, Rev GAT TCC ACT TTG CGT TCA AGG T, FGFR3 Fwd GAG GCC ATC GGC ATT GAC, Rev TGG CAT CGT CTT TCA GCA TCT, GAPDH Fwd GGA CCT GAC CTG CCG TCT AGA A, GAPDH Rev GGT GTC GCT GTT GAA GTC AGA G. FGFR3

primers were located on exon 12 and were designed using Primer Xpress software (Applied Biosystems, Life Technologies).

Orthotopic bladder cancer xenograft model

All animal work was approved by the Institutional Review Board of the University of British Columbia (approval #A08-0733). Six-week-old male nude mice (Harlan Laboratories, Indianapolis, IN) were anesthetized with isoflurane (2 Vol.%) and analgesia was provided by subcutaneous injection with buprenorphine and meloxicam (Boehringer Ingelheim, Burlington, ON). After disinfection of the abdominal wall with chlorhexidine, a low transverse laparotomy was made and the urinary bladder was extra-corporalized. 50μl of a cell suspension containing 2.5×10^5 or 5.0×10^5 cells was inoculated using a 30G needle directly into the bladder wall (24). The incision was closed with suture.

Bioluminescence was used to quantify tumor burden and was measured on the Xenogen IVIS Spectrum imaging system after intraperitoneal injection of 200ug/kg luciferin (Caliper). Images were taken at 10 and 14 min after luciferin injection and the average counts were used for statistical analysis. Bioluminescence imaging was performed on the 5^{th} or 6^{th} day, and mice were divided into equal treatment groups based on tumor burden (13 to 16 animals per group). Treatment started the following day and imaging was repeated every 5 days. Tumor uptake rates in our orthotopic xenograft model were 100% for UM-UC14 and RT112, and 96% for UM-UC1 cells.

In vivo treatment

The FGFR3 targeting antibody R3Mab (21) was provided by Genentech (South San Francisco, CA). It was reconstituted in sterile water for injection at a concentration of 10 mg/ml and stored at 4°C. Control treatments included phosphate buffer saline (PBS) and an isotype control antibody (human IgG1). All agents were prepared freshly in PBS immediately before each treatment session and injected intraperitoneally.

Evaluation of proliferation and apoptosis in orthotopic xenograft tumors

Representative tumors derived from orthotopic xenografts were stained for Ki-67 and caspase-3, as markers of proliferation and apoptosis. Staining of paraffin embedded tumor sections (4mm) was conducted on a Ventana Discovery XT autostainer platform (Ventana Medical Systems, Tuscan, AZ) with an enzyme labeled biotin streptavidin system and a solvent resistant 3,3-Diaminobenzidine (DAB) Map kit by using primary antibodies at a concentration of 1:500 for Ki-67 and 1:50 for caspase-3 at 37°C and an incubation time of 1 hour. After application of the secondary antibody, a hematoxylin counterstain was performed. The average count of positively stained cells in ten high power fields was evaluated on each section.

Statistics

Statistical analysis was carried out using Chi-square testing for analysis of IHC, in addition t-test und ANOVA were performed for *in vitro* and *in vivo* experiments. Significance was defined at values of $P<0.05$. Data were expressed as mean ± standard error, if not differently noted. Statistical analysis was performed using GraphPad Prism 4.03 (GraphPad Software, Inc., La Jolla, CA).

Results

Immunohistochemistry

A human bladder cancer tissue microarray (TMA) containing cores of 153 tumor samples from patients with urothelial carcinoma of the bladder (Tab. 1) was stained for total FGFR3 expression. The median age of these patients was 65 (range 37 to 85) years and 77% were male. Tissue was obtained both from cystectomy and transurethral resection specimens. The intensity of staining was graded from 0 (no staining) to 3 (strong staining). Tumors were classified as invasive (T1-T4 in 68%) or non-invasive (Ta in 32%), and as low (28%) or high (72%) grade. Expression of FGFR3 was found in approximately 70% of both low and high-grade tumors, as well as equally between invasive and non-invasive tumors. High levels (≥2) of FGFR3 were observed in 36% of low grade tumors compared to 22% of high-grade lesions (P=0.047; Fig. 1A). No significant difference was found for invasive vs. non-invasive tumors. There was no evidence of staining in normal urothelium.

Mutation analysis

170 fresh frozen samples from an independent cohort of patients with urothelial carcinoma of the bladder were analyzed for mutations in the FGFR3 gene by direct sequencing. The median age of the patients was 66 (range 41-87) years and 77% were male. The stage and grade of tumors are reflected in Tab. 2. FGFR3 mutations in exon 7 or exon 10 were found in 26% of all samples and 56% of low-grade tumors. Low grade, non-invasive tumors showed more than a fourfold increased rate of FGFR3 mutation compared to high grade, invasive tumors (Tab. 2). Similar analysis revealed a S249C mutation (exon 7) in 5 of 19 cell lines and a Y375C (exon 10) mutation in one cell line. The remaining cell lines contained a wild-type FGFR3 gene (Tab. 2).

Expression of FGFR3 in bladder cancer cell lines in relation to epithelial/mesenchymal markers

A panel of 12 human bladder cancer cell lines was screened for RNA and protein expression of FGFR3 by qPCR and Western blot. Based on prior work linking growth factor receptor activity to epithelial-to-mesenchymal (EMT) differentiation and invasive potential of bladder cancer cell lines, the panel was divided in non-invasive/epithelial cell lines and invasive/mesenchymal cell lines (25). Expression of FGFR3 was associated with detection of E-Cadherin, a marker of epithelial differentiation. Mesenchymal cell lines, defined by expression of ZEB-1 and Vimentin and loss of E-cadherin, demonstrated lower levels of FGFR3 (Fig. 1B and C).

In vitro targeting of FGFR3

FGFR3 pathway activity was verified in UM-UC1 urothelial cancer cells, which express a high level of wild-type FGFR3. Stimulation of these cells with the ligand FGF-1 resulted in phosphorylation of FGFR3 and activation of the downstream signaling cascade in a time dependent manner. Phosphorylation of the receptor was followed by phosphorylation of FRS-2, and increasing activation of both p-Erk 1/2 and p-Akt (Fig. 2A). In the same cell lines, inhibition of FGFR3 with R3Mab abrogated receptor phosphorylation, as well as phosphorylation of FRS-2 and Erk1/2 (Fig 2B). A similar experiment was performed in UM-UC14, which harbors an S249C mutation in exon 7 of FGFR3, but here an immune-precipitation was performed with anti-FGFR3 and subsequent blotting with anti-phospho-tyrosine as an alternative method to demonstrate FGFR3 phosphorylation (Fig. 2C). Treatment with R3Mab in regular growth medium resulted in a concentration-dependent growth inhibition in three out of four different tumor cell lines in a crystal violet assay (Fig. 2D). UM-UC1 displayed the most pronounced anti-proliferative response, while the highly

mesenchymal and invasive cells UM-UC3, UM-UC13, T24 and 253J-BV, all of which do not express appreciable levels of FGFR3, showed no response. RT4V6, RT112 (both high expression of wild-type FGFR3), UM-UC16 (low expression of ^{S249C}FGFR3) and UM-UC14 (modest expression of ^{S249C}FGFR3) showed only modest response.

In vivo treatment of orthotopic bladder cancer xenografts

UM-UC14, RT112 and UM-UC1 cells were orthotopically injected into the bladder wall of athymic nude mice. Successful tumor inoculation was verified by bioluminescence imaging on the 5th or 6th day and the mice were divided into equal groups based on tumor burden. They were then treated with active agent (R3Mab) or control every 72 hours and bioluminescence was repeated every 5 days.

Two different dose levels were tested in UM-UC14 xenografts, including 15 mg/kg and 30 mg/kg and compared to a saline treated group (IgG1 control not available for this experiment). Tumor growth, 30 days after inoculation, showed a dose-dependent inhibition of tumor growth with a reduction in tumor growth of 22% and 33%, respectively (Fig. 3A). Evaluation of representative tumor samples harvested from this experiment demonstrated inhibition of FGFR3 phosphorylation by immunoprecipitation of FGFR3 and subsequent immunoblotting with anti-phospho-tyrosine (Fig. 3B).

In mice bearing orthotopic RT112 xenografts, R3Mab treatment at a dose of 30 mg/kg was compared to both a saline control group and a non-targeting human IgG1-control. The IgG1 had no effect on tumor growth, while mice treated with R3Mab showed a reduction in tumor growth by 59.2 % compared to IgG and 57.2% compared to saline controls (Fig. 3C).

In vivo, UM-UC1 tumors orthotopically injected into the bladder of nude mice showed a reduction in tumor growth of 83.9% when treated with R3Mab compared to mice injected with IgG and 84,1 % compared to saline controls (Fig. 4A and B). Evaluation of whole bladder samples by Western blotting at the end of the experiment showed a significant inhibition of FGFR3 phosphorylation and downstream signaling, including p-FRS2, p-ERK1/2, cyclin D1 and cyclin E (Fig. 4C). Overall this indicates that the observed tumor growth reduction is due to highly effective FGFR3 pathway inhibition by R3Mab *in vivo* (Fig. 4D). The inhibition of tumor growth is related to anti-proliferative effects of R3Mab expressed in a reduced Ki-67 proliferative index (Fig. 4E), while no difference has been observed for expression of cleaved caspase-3 in xenograft tumors (data not shown) as a marker for apoptosis.

Discussion

We have demonstrated a high rate of FGFR3 mutation and over-expression in an American cohort of patients. We have also shown that FGFR3 signaling is active in pre-clinical models of bladder cancer, and that specific inhibition of FGFR3 with a monoclonal antibody induces growth arrest in orthotopic bladder cancer xenografts. Our data builds on prior experience with the same inhibitor in subcutaneous models (21), yet advances this therapeutic strategy to meet a significantly higher bar of efficacy in the orthotopic setting. We believe that this provides the proof of principle required to investigate this agent or a similar novel FGFR3 inhibitor in specific clinical trials for bladder cancer.

We see a lower rate of FGFR3 mutations in low grade tumors (4, 26, 27) and a higher rate of FGFR3 overexpression in high grade tumors (5) compared to prior reports. This is most likely related to patient selection, which in turn is a reflection of the highly specialized clinical setting in which these tumor samples were collected. There are also likely

differences in IHC methodology and assessment of staining. A slight increase in mutation rate would be expected if exon 15 had also been assessed.

A limitation of current pre-clinical models of bladder cancer is the inability to model low grade, non-invasive disease. Although we possess bladder cancer cell lines with FGFR3 mutations, these mutations are found only in highly invasive cell lines that are not representative of non-muscle invasive disease. RT4 is the only cell line that is low grade, but even it is invasive and it expresses wild type FGFR3. Our data therefore do not allow us to draw any conclusions about the potential efficacy of FGFR3 inhibition in non-muscle invasive bladder cancer. We have tested tyrosine kinase inhibitors targeting FGFR3 in RT4v6 with excellent growth inhibition (data not shown). We and others are developing primary xenografts using fresh patient samples in an attempt to overcome our inability to model non-muscle invasive disease.

The optimal disease state to test FGFR3 inhibition is open to debate. While it would seem logical to target the activating mutations in non-muscle invasive disease, it will be challenging to give systemic therapy to this patient population, especially since FGFR3 mutations indicate a favorable prognosis (8, 28, 29). A trial with gefitinib (an oral EGFR inhibitor) failed to accrue patients in Canada at least in part because physicians and patients did not accept systemic therapy for NMIBC (NCT00352079). The currently available multi-tyrosine kinase inhibitors that target FGFR3 are all marred with concerns regarding systemic toxicity that would severely limit their use in this setting (11). R3Mab may prove to be better tolerated, since it should avoid the hypophosphatemia and soft-tissue calcification associated with pan-FGFR inhibitors. It remains to be proven whether these agents and especially R3Mab are efficacious when administered intravesically.

Our results suggest that R3Mab should be tested in patients with muscle invasive bladder cancer whose tumors demonstrate FGFR3 over-expression. There is a pressing need for new treatments in this lethal variant of bladder cancer, and our findings would support testing FGFR3 inhibition in conjunction with systemic cytotoxic chemotherapy. Whether FGFR3 mutations are relevant in the context of muscle invasive bladder cancer remains to be shown. Our cell line investigations reveal little drug activity in invasive cells with FGFR3 mutations, with the exception of UM-UC14. We observed a reduced growth inhibitory effect in UM-UC14 compared to prior reports (21, 30). This may be a difference in the model systems (orthotopic vs. heterotopic) or potentially related to phenotypic drift in different strains of UM-UC14. Regardless of cell line data, any clinical trial would have to include assessment of FGFR3 mutation status and expression in every tumor. Patient selection based on these parameters may be an important factor in subsequent patient selection. We are also investigating mechanisms of resistance to R3Mab in pre-clinical models with the intention of potentially using this information for patient enrichment in clinical trials. Since FGFR3 appears to drive growth through AKT and ERK1/2 (31), it is likely that there is redundancy with other growth factor receptor pathways (32) much as we have described with EGFR and PDGFR-ß (33).

We have confirmed the results of prior reports on FGFR3 mutation and expression patterns in urothelial carcinoma of the bladder: FGFR3 is frequently mutated in non-invasive bladder cancer and frequently over-expressed in both non-invasive and invasive bladder cancer. We have demonstrated that targeting FGFR3 with a specific inhibitory monoclonal antibody (R3Mab) effectively abrogates FGFR3 signaling pathway activation with a resultant decrease in tumor growth. This inhibitor is highly efficacious in a selection of bladder cancer cell lines and orthotopic xenografts. These are promising results that warrant translation into clinical trials in patients with bladder cancer.

Acknowledgments

The authors are particularly grateful to Eliana Beraldi for her assistance with viral transduction of cell lines. In addition, we would like to thank Ladan Fazli and Estelle Li for their work on Ki-67 and Caspase-3 expression on xenograft tumor sections.

Grant Support: Grant funding was provided through a National Cancer Center Core Grant (The University of Texas, M.D. Anderson Cancer Center).

In addition P.C. Black has been awarded a Developmental Grant from the NIH GU SPORE in bladder cancer at MD Anderson Cancer Center (CA91846), a NIH T32 Training Grant, an AUA Foundation Grant and a Mentored Physician Scientist Award from Vancouver Coastal Health Research Institute.

References

1. American Cancer Society. [Last accessed September 24, 2012] Cancer Facts and Figures 2012. Available online2012
2. Pashos CL, Botteman MF, Laskin BL, Redaelli A. Bladder cancer: epidemiology, diagnosis, and management. Cancer Pract. 2002; 10:311–22. [PubMed: 12406054]
3. Avritscher EB, Cooksley CD, Grossman HB, Sabichi AL, Hamblin L, Dinney CP, et al. Clinical model of lifetime cost of treating bladder cancer and associated complications. Urology. 2006; 68:549–53. [PubMed: 16979735]
4. Billerey C, Chopin D, Aubriot-Lorton MH, Ricol D, Gil Diez de Medina S, Van Rhijn B, et al. Frequent FGFR3 mutations in papillary non-invasive bladder (pTa) tumors. Am J Pathol. 2001; 158:1955–9. [PubMed: 11395371]
5. Mhawech-Fauceglia P, Cheney RT, Fischer G, Beck A, Herrmann FR. FGFR3 and p53 protein expressions in patients with pTa and pT1 urothelial bladder cancer. Eur J Surg Oncol. 2006; 32:231–7. [PubMed: 16412606]
6. Tomlinson DC, Baldo O, Harnden P, Knowles MA. FGFR3 protein expression and its relationship to mutation status and prognostic variables in bladder cancer. J Pathol. 2007; 213:91–8. [PubMed: 17668422]
7. van Oers JM, Wild PJ, Burger M, Denzinger S, Stoehr R, Rosskopf E, et al. FGFR3 mutations and a normal CK20 staining pattern define low-grade noninvasive urothelial bladder tumours. Eur Urol. 2007; 52:760–8. [PubMed: 17240035]
8. van Rhijn BW, Vis AN, van der Kwast TH, Kirkels WJ, Radvanyi F, Ooms EC, et al. Molecular grading of urothelial cell carcinoma with fibroblast growth factor receptor 3 and MIB-1 is superior to pathologic grade for the prediction of clinical outcome. J Clin Oncol. 2003; 21:1912–21. [PubMed: 12743143]
9. Bakkar AA, Wallerand H, Radvanyi F, Lahaye JB, Pissard S, Lecerf L, et al. FGFR3 and TP53 gene mutations define two distinct pathways in urothelial cell carcinoma of the bladder. Cancer Res. 2003; 63:8108–12. [PubMed: 14678961]
10. Tomlinson DC, Hurst CD, Knowles MA. Knockdown by shRNA identifies S249C mutant FGFR3 as a potential therapeutic target in bladder cancer. Oncogene. 2007; 26:5889–99. [PubMed: 17384684]
11. Turner N, Grose R. Fibroblast growth factor signalling: from development to cancer. Nat Rev Cancer. 2010; 10:116–29. [PubMed: 20094046]
12. Trudel S, Li ZH, Wei E, Wiesmann M, Chang H, Chen C, et al. CHIR-258, a novel, multitargeted tyrosine kinase inhibitor for the potential treatment of t(4;14) multiple myeloma. Blood. 2005; 105:2941–8. [PubMed: 15598814]
13. Lamont FR, Tomlinson DC, Cooper PA, Shnyder SD, Chester JD, Knowles MA. Small molecule FGF receptor inhibitors block FGFR-dependent urothelial carcinoma growth in vitro and in vivo. Br J Cancer. 2011; 104:75–82. [PubMed: 21119661]
14. Rebouissou S, Herault A, Letouze E, Neuzillet Y, Laplanche A, Ofualuka K, et al. CDKN2A homozygous deletion is associated with muscle invasion in FGFR3-mutated urothelial bladder carcinoma. J Pathol. 2012; 227:315–24. [PubMed: 22422578]

15. Chen J, Lee BH, Williams IR, Kutok JL, Mitsiades CS, Duclos N, et al. FGFR3 as a therapeutic target of the small molecule inhibitor PKC412 in hematopoietic malignancies. Oncogene. 2005; 24:8259–67. [PubMed: 16091734]
16. Jonker DJ, Rosen LS, Sawyer MB, de Braud F, Wilding G, Sweeney CJ, et al. A phase I study to determine the safety, pharmacokinetics and pharmacodynamics of a dual VEGFR and FGFR inhibitor, brivanib, in patients with advanced or metastatic solid tumors. Annals of oncology : official journal of the European Society for Medical Oncology / ESMO. 2011; 22:1413–9. [PubMed: 21131369]
17. Kim KB, Chesney J, Robinson D, Gardner H, Shi MM, Kirkwood JM. Phase I/II and pharmacodynamic study of dovitinib (TKI258), an inhibitor of fibroblast growth factor receptors and VEGF receptors, in patients with advanced melanoma. Clin Cancer Res. 2011; 17:7451–61. [PubMed: 21976540]
18. Ratain MJ, Schwartz GK, Oza AM, Rudin CM, Kaye SB, De Jonge MJ, et al. Brivanib (BMS-582664) in advanced solid tumors (AST): Results of a phase II randomized discontinuation trial (RDT). J Clin Oncol. 2011; 29(suppl) abstr 3079.
19. Brooks AN, Kilgour E, Smith PD. Molecular pathways: fibroblast growth factor signaling: a new therapeutic opportunity in cancer. Clin Cancer Res. 2012; 18:1855–62. [PubMed: 22388515]
20. Chesi M, Nardini E, Brents LA, Schrock E, Ried T, Kuehl WM, et al. Frequent translocation t(4;14)(p16.3;q32.3) in multiple myeloma is associated with increased expression and activating mutations of fibroblast growth factor receptor 3. Nat Genet. 1997; 16:260–4. [PubMed: 9207791]
21. Qing J, Du X, Chen Y, Chan P, Li H, Wu P, et al. Antibody-based targeting of FGFR3 in bladder carcinoma and t(4;14)-positive multiple myeloma in mice. J Clin Invest. 2009; 119:1216–29. [PubMed: 19381019]
22. Jebar AH, Hurst CD, Tomlinson DC, Johnston C, Taylor CF, Knowles MA. FGFR3 and Ras gene mutations are mutually exclusive genetic events in urothelial cell carcinoma. Oncogene. 2005; 24:5218–25. [PubMed: 15897885]
23. Cheng B, Fu XB, Sheng ZY, Sun TZ, Sun XQ. [A comparative study of EGFR and FGFR-2 expression in fetal and adult skin]. Zhonghua zheng xing wai ke za zhi = Zhonghua zhengxing waike zazhi = Chinese journal of plastic surgery. 2003; 19:91–4. [PubMed: 12889182]
24. Dinney CP, Fishbeck R, Singh RK, Eve B, Pathak S, Brown N, et al. Isolation and characterization of metastatic variants from human transitional cell carcinoma passaged by orthotopic implantation in athymic nude mice. J Urol. 1995; 154:1532–8. [PubMed: 7658585]
25. Black PC, Brown GA, Inamoto T, Shrader M, Arora A, Siefker-Radtke AO, et al. Sensitivity to epidermal growth factor receptor inhibitor requires E-cadherin expression in urothelial carcinoma cells. Clin Cancer Res. 2008; 14:1478–86. [PubMed: 18316572]
26. van Rhijn BW, Montironi R, Zwarthoff EC, Jobsis AC, van der Kwast TH. Frequent FGFR3 mutations in urothelial papilloma. J Pathol. 2002; 198:245–51. [PubMed: 12237885]
27. Neuzillet Y, Paoletti X, Ouerhani S, Mongiat-Artus P, Soliman H, de The H, et al. A meta-analysis of the relationship between FGFR3 and TP53 mutations in bladder cancer. PLoS One. 2012; 7:e48993. [PubMed: 23272046]
28. van Rhijn BW, Lurkin I, Radvanyi F, Kirkels WJ, van der Kwast TH, Zwarthoff EC. The fibroblast growth factor receptor 3 (FGFR3) mutation is a strong indicator of superficial bladder cancer with low recurrence rate. Cancer Res. 2001; 61:1265–8. [PubMed: 11245416]
29. Hernandez S, Lopez-Knowles E, Lloreta J, Kogevinas M, Amoros A, Tardon A, et al. Prospective study of FGFR3 mutations as a prognostic factor in nonmuscle invasive urothelial bladder carcinomas. J Clin Oncol. 2006; 24:3664–71. [PubMed: 16877735]
30. Masson-Lecomte A, Vordos D, de la Taille A, Neuzillet Y, Radvanyi F, Allory Y. [Update on FGFR3 mutation and MRES phenotype in urothelial carcinogenesis]. Progres en urologie : journal de l'Association francaise d'urologie et de la Societe francaise d'urologie. 2013; 23:96–8.
31. Askham JM, Platt F, Chambers PA, Snowden H, Taylor CF, Knowles MA. AKT1 mutations in bladder cancer: identification of a novel oncogenic mutation that can co-operate with E17K. Oncogene. 2010; 29:150–5. [PubMed: 19802009]

32. Stommel JM, Kimmelman AC, Ying H, Nabioullin R, Ponugoti AH, Wiedemeyer R, et al. Coactivation of receptor tyrosine kinases affects the response of tumor cells to targeted therapies. Science. 2007; 318:287–90. [PubMed: 17872411]

33. Black PC, Brown GA, Dinney CP, Kassouf W, Inamoto T, Arora A, et al. Receptor heterodimerization: a new mechanism for platelet-derived growth factor induced resistance to anti-epidermal growth factor receptor therapy for bladder cancer. J Urol. 2011; 185:693–700. [PubMed: 21168861]

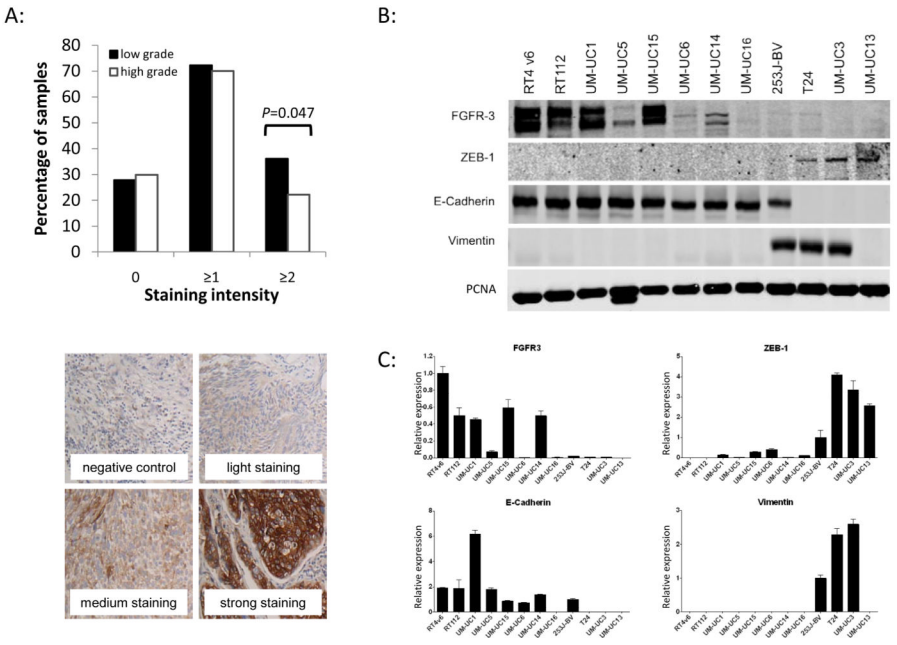

Fig. 1.

A: Tissue microarray analysis for total FGFR3 expression. A TMA was stained for FGFR3 expression with a human specific FGFR3 antibody. Staining was semi-quantitative analyzed and staining intensity assessed between 0 (no staining) and 3 (intensive staining). Average staining intensity was analyzed for tumor grade. One sided chi-square test was performed and revealed a significant overexpression (P=0.047) of FGFR3 in low grade tumors compared to high grade tumors with a positive staining in 36% and 22% percent of tumors, respectively. The percentages of patients with the specified staining intensities add up to >100% because the ≥1 and ≥2 intensity groups overlap. **B:** Western blot analysis of FGFR3 in relation to epithelial and mesenchymal markers in a panel of urothelial cancer cell lines. **C:** qPCR analysis for FGFR3 in relation to epithelial and mesenchymal markers in a panel of urothelial cancer cell lines. Expression of total FGFR3 is associated with an epithelial phenotype of cell lines. Epithelial cell lines defined by expression of E-Cadherin show higher levels of FGFR3 than mesenchymal cell lines characterized by loss of E-Cadherin and expression of ZEB-1 and Vimentin.

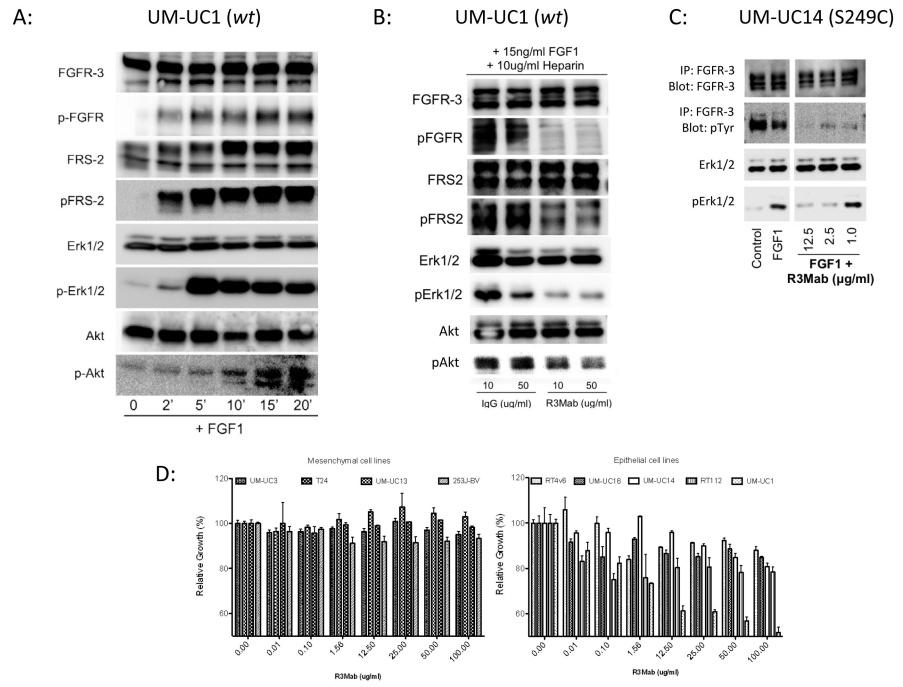

Fig. 2.

A: Activation of FGFR3 signaling cascade in wild-type (wt) FGFR3 harboring cell lines UM-UC1 by stimulation with fibroblast growth factor (FGF)-1. Cells were cultured in regular growth medium on 6 cm culture dishes to about 50% confluence. Cells were starved in serum free media for 24 hours. Growth medium was exchanged to medium supplemented with FGF-1 at a concentration of 10ng/ml. Cells were then harvested on ice according to the time point of 2, 5, 10, 15 and 20 minutes after stimulation. Cells were lysed with RIPA buffer including proteinase and phosphatase inhibitor and 60 ug of total protein used. Indicating for an activation of the FGFR3 signaling cascade is shown by a time dependent increase of phospho-FGFR, followed by phosphorylation of FRS-2, ERK-1/2 and Akt. Inhibition of FGFR3 signaling by the FGFR3 specific inhibitory antibody R3Mab in wt-FGFR3 harboring UM-UC1 cells and the S249C mutant FGFR3 bearing cell lines UM-UC14. **B:** UM-UC1 cells were plated in normal growth media and allowed to attach for 24 hours, then washed two times with PBS and then starved in media without FBS for 24 hours, followed by stimulation with FGF-1 (15ng/ml) for 10 min in the presence of Heparin (10 ug/ml). Either human control IgG or R3Mab was added in serum free media at concentrations of 10 and 50 ug/ml. Phosphorylation of FGFR, FRS2, Erk1//2 and Akt was evaluated by Western blot and demonstrates lower phosphorylation levels under treatment with R3Mab. **C:** A strong auto-phosphorylation of FGFR3 is found in UM-UC14 cells in regular growth conditions. R3Mab blocks auto-phosphorylation of $FGFR3^{S249C}$ receptor even under stimulated conditions with supplemented FGF1, while Erk1/2 shows increased levels of phosphorylation under stimulation with FGF1 and at low concentrations of R3Mab (1 ug/ml). **D:** *In vitro* growth inhibition of R3Mab on urothelial cancer cell lines. Cell lines were grown under to 50% confluence in regular growth medium. R3Mab was then added to growth medium and growth inhibition was evaluated by crystal violet staining after 48 hours of treatment with FGFR3 specific inhibitory antibody. Mesenchymal cell lines with low expression of FGFR3 show no specific response to treatment with R3Mab at concentrations up to 100 ug/ml, while epithelial cell lines with high expression of FGFR3 show a growth inhibition of up to 50%, as observed in UM-UC1 cells, a cell line derived from a lymph node metastasis from an urothelial carcinoma.

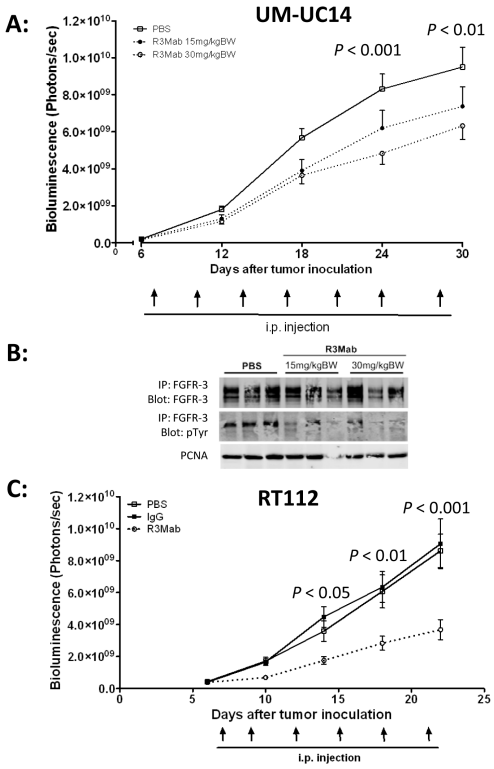

Fig. 3.

A: Dose-dependent growth inhibition of orthotopic UM-UC14 xenografts. Constitutively activated, mutant FGFR3^{S249C} harboring UM-UC14 cells were inoculated orthotopically in bladder of nude mice. Mice were subdivided into three treatment arms: IgG control (N=14), R3Mab 15 mg/kgBW (N=13) and R3Mab 30 mg/kgBW (N=13). Systemic, intraperitoneal (i.p.) applied treatment with R3Mab results in a dose-dependent growth inhibition compared to non-specific IgG control treatment. Tumor growth was evaluated by bioluminescent imaging. **B:** Western blot analysis of tumor samples, derived from orthotopically grown UM-UC14 xenografts after treatment with R3Mab at 15 mg/kgBW and 30 mg/kgBW. Tumors treated with R3Mab demonstrate lower phosphorylation levels indicated by reduced pTyr, while levels of total FGFR3 in the different treatment and control groups are unchanged. **C:** Tumor growth inhibition of orthotopic RT112 xenografts. Wild-type FGFR3 harboring RT112 cells were inoculated orthotopically in bladder of nude mice. Mice received either 30 mg/kgBW R3Mab (N=15), non-targeting IgG control (N=15) or PBS (N=15) as a negative control. I.p. treatment with R3Mab results in significant inhibition of tumor growth compared to saline treated mice as well as mice in the IgG control arm. Tumor growth was evaluated by bioluminescent imaging.

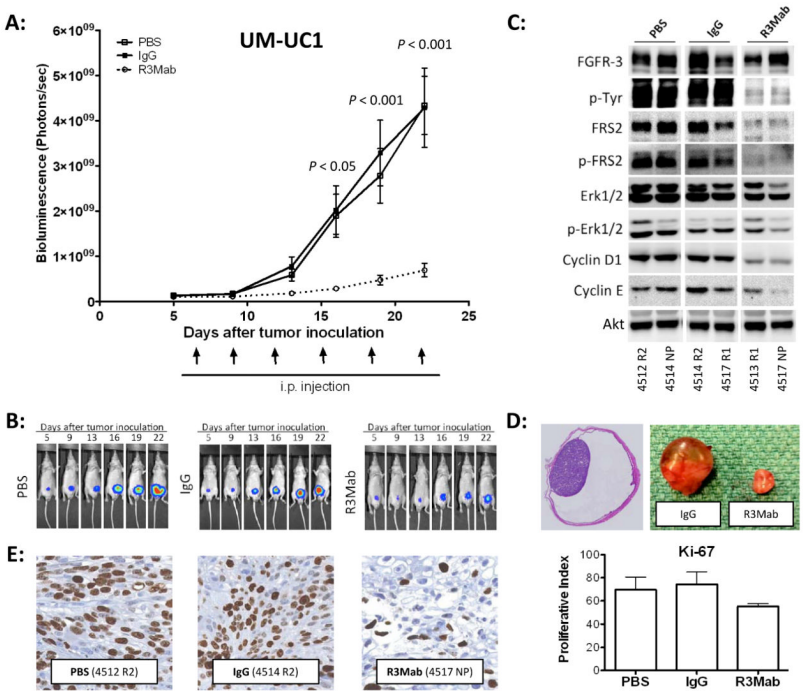

Fig. 4.

A: Tumor growth inhibition of orthotopic UM-UC1 xenografts. Wild-type FGFR3 harboring UM-UC1 cells were inoculated orthotopically in bladder of nude mice. Mice were assigned to three groups receiving either PBS as control (N=16), non-targeting human-IgG (N=13) or R3Mab at a dose of 30 mg/kgBW (N=14). I.p. treatment with R3Mab resulted in significant inhibition of tumor growth compared to saline treated mice as well as mice in the IgG control arm. Tumor growth was evaluated by bioluminescent imaging. **B:** Bioluminescent images of orthotopic UM-UC1 xenografts. Mice were imaged on day 5 after tumor inoculation and grouped into the different treatment arms. Pictures show representative mice of the three treatment groups: PBS (saline), IgG controls und R3Mab treated mice. **C:** Western blot analysis orthotopically implanted UM-UC1 xenografts. Tumors were collected at the endpoint of the experiment (day 22) and snap frozen. Random tumors of the treatment groups were lysed and total protein blotted for members of the FGFR3 signaling cascade. R3Mab treated tumors show a significant reduced activation of FGFR3 signaling with downregulation of FRS2, lower phosphorylation levels of p-Erk 1/2 and lower expression of Cyclin D1 and Cyclin E. **D:** Orthotopic xenografts. Full section of an orthotopically implanted bladder tumor (left). Representative tumors of orthotopic UM-UC1 xenografts treated with R3Mab or control saline at day 22 after tumor inoculation (right). **E:** Evaluation of xenograft tumor sections for Ki-67 staining revealed a lower proliferative index for R3Mab treated UM-UC1 tumors than control tumors, treated with either PBS or non-targeting human IgG.

Table 1

Patient and tumor characteristics for tissue microarray analysis

	Male [*N* (%)]	**Female [*N* (%)]**
Age (Mean, Range)	65 (37-85)	67 (40-81)
N	112 (77)	33 (23)
G1	1 (1)	0 (0)
G2	35 (31)	4 (12)
G3	76 (68)	29 (88)
papillary	47 (42)	13 (39)
non-papillary	65 (58)	20 (61)
NMIBC[*]	40 (36)	7 (21)
MIBC[**]	72 (64)	26 (79)

[*] non-muscle invasive bladder cancer

[**] muscle invasive bladder cancer

Table 2

FGFR3 mutation analysis of tumor samples and urothelial carcinoma cell lines.

Tumor samples			
	Low grade	**High grade**	**Total**
Non-invasive	28/50 = 56%	2/18 = 11%	30/68 = 46%
Invasive	4/7 = 57%	10/95 = 11%	14/102 = 22%
Total	32/57 = 56%	12/113 = 11%	44/170 = 26%
Exon 7 mutation: 31 (70%)		Exon 10 mutation: 13 (30%)	
Exon	***Nucleotide position / base change***	***Codon / change in amino acid***	***N***
7	746 C>G	S249C	31
10	1114 G>T	G372C	4
10	1117 A>T	S373C	1
10	1124 A>G	Y375C	7
10	1156 T>C	F386L	1

Cell lines					
Cell line	***Exon 7***	***Exon 10***	***Cell line***	***Exon 7***	***Exon 10***
253J-P	wt	wt	UM-UC7	wt	wt
253J-BV	wt	wt	UM-UC10	wt	wt
RT4 v6	wt	wt	UM-UC11	wt	wt
RT112	wt	wt	UM-UC12	wt	wt
T24	wt	wt	UM-UC13	wt	wt
UM-UC1	wt	wt	UM-UC14	**S249C**	wt
UM-UC3	wt	wt	UM-UC15	**S249C**	**Y375C**
UM-UC4	wt	wt	UM-UC16	**S249C**	wt
UM-UC5	wt	wt	UM-UC17	**S249C**	wt
UM-UC6	**R248C**	wt			